REVIEW ARTICLE

Imaging techniques for tumour delineation and heterogeneity quantification of lung cancer: overview of current possibilities

Wouter van Elmpt[1], Catharina M.L. Zegers[1], Marco Das[2], Dirk De Ruysscher[3]

[1]Department of Radiation Oncology (MAASTRO), [2]Department of Radiology, GROW, School for Oncology and Developmental Biology, Maastricht University Medical Centre, Maastricht, The Netherlands; [3]Radiation Oncology, University Hospitals Leuven/KU Leuven, Leuven, Belgium

ABSTRACT Imaging techniques for the characterization and delineation of primary lung tumours and lymph nodes are a prerequisite for adequate radiotherapy. Numerous imaging modalities have been proposed for this purpose, but only computed tomography (CT) and FDG-PET have been implemented in clinical routine. Hypoxia PET, dynamic contrast-enhanced CT (DCE-CT), dual energy CT (DECT) and (functional) magnetic resonance imaging (MRI) hold promise for the future. Besides information on the primary tumour, these techniques can be used for quantification of tissue heterogeneity and response. In the future, treatment strategies may be designed which are based on imaging techniques to optimize individual treatment.

KEY WORDS Lung cancer; imaging; tumour delineation; heterogeneity

J Thorac Dis 2014;6(4):319-327. doi: 10.3978/j.issn.2072-1439.2013.08.62

Introduction

Lung cancer is the single most important cause of cancer deaths in all developed countries (1). In the upcoming countries such as China, it is expected that lung cancer will have epidemic proportions within a few decades (2). Radiotherapy plays an increasing role in all stages of lung cancer: stage I non-small cell lung cancer (NSCLC) is treated with stereotactic body radiotherapy (SBRT) (3), also called stereotactic ablative radiotherapy or SABR with results that equal those of surgery. Stage III NSCLC and small cell lung cancer (SCLC) is most often treated with combined chemotherapy and radiotherapy and patients with oligometastases may experience long-term disease-free survival with treatment that includes radiotherapy (4,5).

However, a thorough definition of the tumour to be irradiated is a prerequisite for successful radiotherapy. Visualisation of the tumour boundaries using morphological imaging techniques such as computed tomography (CT) or magnetic resonance imaging (MRI) are of importance, but also the biological characteristics of the cancer and of the organs at risk (OAR) can nowadays be visualized using molecular imaging e.g., positron emission tomography (PET) techniques. Assessment of this biological heterogeneity of tumours using imaging may lead to more individualized therapy. Using the knowledge of characteristics of the tumour and of the OARs should enable an optimised therapeutic ratio. Although seemingly obvious, reality shows that achieving this goal has been proven to be difficult. Definition of the tumour boundaries with high accuracy and low inter- and intra-observed variability is hampered by the lack of validated automated systems that work well for complicated volumes that are surrounded by OARs with similar densities. Biological characteristics can be imaged, but their implementation in standard practice requires prospective clinical studies showing improved outcomes.

The present manuscript will focus on the delineation and characterization of primary tumour and lymph node involvement in lung cancer patients using the latest available imaging techniques. Some of these techniques are already applied in clinical practice and some of them are still on a research level. Furthermore, an outlook is given how to use these methods in the future to individualize lung cancer treatment and to optimize the balance between local tumour control and organ toxicity.

Correspondence to: Wouter van Elmpt, Ph.D. Department of Radiation Oncology (MAASTRO), GROW, School for Oncology and Developmental Biology, Maastricht University Medical Centre, Dr. Tanslaan 12, NL-6229 ET Maastricht, The Netherlands. Email: wouter.vanelmpt@maastro.nl.

Submitted Aug 05, 2013. Accepted for publication Aug 21, 2013.
Available at www.jthoracdis.com

ISSN: 2072-1439

Imaging modalities for target volume delineation and quantification

FDG-PET/CT

The accuracy of FDG-PET is higher than CT for the staging of mediastinal lymph nodes in advanced stage lung cancer. Hence, the incorporation of PET in the treatment planning process of radiotherapy is logical. In many planning studies in NSCLC, the use of FDG-PET has resulted in a decrease of the irradiated volumes of the OARs, which may lead to less side effects or to the possibility of radiation dose-escalation with the aim to improve local tumour control (6,7). Prospective studies both in NSCLC and in SCLC indeed showed that selective mediastinal node irradiation based on FDG-PET scans did not lead to higher isolated nodal recurrences (8-10).

The use of FDG-PET in radiotherapy planning was shown to reduce variability of tumour delineation amongst radiation oncologists and allows automatic tumour delineation that can be followed with manual editing if required (11-13). To use PET/CT equipment directly for radiotherapy treatment planning purposes, some additional criteria have to be considered. A detailed overview on the basic technical aspects and recommendations for radiotherapy treatment planning is described in Thorwarth *et al.* (14). On a standard 3D PET/CT acquisition, small lesions might be difficult to detect due to the intrinsic blurring of breathing motion and might also lead to inaccurate quantification of the standardized uptake value (SUV) compared to respiratory correlated 4D acquisitions (15). PET/CT scanners have options for acquiring the images in a respiration correlated (4D) mode to compensate for breathing motion in thorax. Furthermore, several publications have shown that 4D PET indeed improves lesion detectability (16,17). The 4D scan is usually reconstructed as a set of 5, 8 or 10 3D PET/CT scans representing the different phases of the respiratory cycle (18). Acquiring such a 4D PET scan together with a 4D CT scan is however not yet widely implemented in practice. A drawback of the 4D image acquisition is the somewhat prolonged acquisition times that might limit throughput on the PET/CT scanners and not all software systems are able to visualize this large amount of imaging data. However by using more advanced reconstruction algorithms that use only the part of the acquisition without breathing motion (e.g., the exhale phase) (19,20) or (non-rigidly) register the various breathing phases of the PET image to a single image (21) the workflow might be improved.

Tumour delineation for radiotherapy treatment planning purposes is a time-consuming manual procedure that is associated with a lot of intra- and inter-observer variability (22). Although the use of strict delineation protocols decrease variability (23), the time investment for delineation still remains and is limiting for adaptation protocols as well. As in radiotherapy the CT scan is used as the primary dataset because of the accurate quantification of (electron) density necessary for the dose calculation of the radiotherapy treatment plan, automatic segmentation based on CT scans are logical. Moreover, 4D-CT scans have been implemented in routine practice and this movement information can readily be accounted for in automatic delineation protocols. On the other hand, FDG-PET scans do correlate better with anatomical boundaries than CT if the tumour is surrounded by lung (24). Combining CT and FDG-PET is therefore logical and automatic segmentation methods could reduce delineation time. However, only few studies have validated their automated segmentation method with pathology (22,25-28) and there is a lack of technical validation and accuracy as well (29,30). Fully automated tumour segmentation has therefore not been implemented in routine clinical practice.

Hypoxia PET

Tumour cell hypoxia is a known characteristic of solid tumour lesions, which negatively influences treatment efficacy (31). Accurate identification of tumour hypoxia is of importance to select patients which will benefit from specific anti-hypoxic treatments. The use of the Eppendorf electrode is the gold standard to assess tumour hypoxia, however this method has the disadvantage to be invasive, limiting its use to well accessible superficial tumours (32). Hypoxia PET imaging allows a non-invasive detection and quantification of tumour hypoxia and it provides the opportunity to display the spatial distribution of hypoxia, which is essential for its integration in radiation dose distribution. The most common mechanism to detect tumour hypoxia is the use of 2-nitroimidazoles PET tracers which show a selective binding and retention in the hypoxic tumour cells.

Several 2-nitroimidazoles, labelled with fluor-18 [^{18}F], have already been applied in patients to identify hypoxia. The first and most familiar hypoxia PET tracer is [^{18}F]MISO, however, a slow accumulation in the hypoxic lesions and limited normal tissue clearance limits its clinical use (33). Therefore, alternative tracers are developed to improve the pharmacokinetic properties of the hypoxia tracer by enhancing the hydrophilicity and clearance of the tracer, examples are [^{18}F]AZA, [^{18}F]ETNIM, [^{18}F]EF3, [^{18}F]HX4 and the nucleoside conjugate Cu-ATSM.

Quantification of tumour hypoxia based on PET imaging can be performed on static images, acquired at a certain time-point post-injection, or based on dynamic acquisitions, which takes also perfusion of the lesion into account (34). Figure 1 shows an

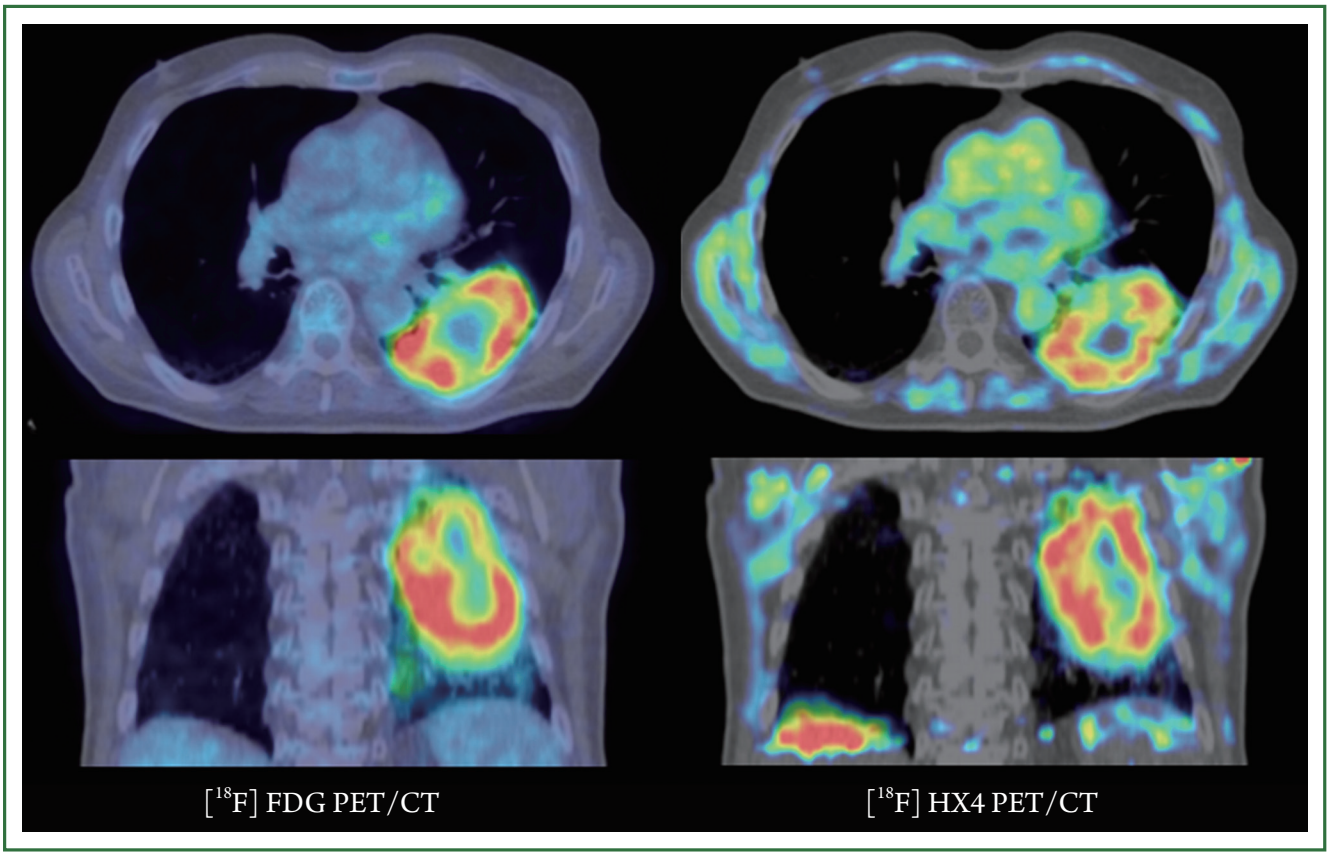

Figure 1. Example of a NSCLC patient having both an FDG-PET/CT scan (left) and a hypoxia HX4-PET/CT scan. Clearly visible is the tumour heterogeneity both on the metabolic (FDG) and hypoxic (HX4) PET image.

example of a lung cancer patient having both an FDG-PET/CT scan and an hypoxia [^{18}F]HX4-PET/CT scan. In NSCLC patients, hypoxia PET has shown to be correlated with prognosis and to give different information than FDG uptake (35,36). Studies with hypoxia PET imaging show the presence of tumour cell hypoxia in the majority of NSCLC lesions (37-40). The extent of tumour hypoxia correlates with tumour response and risk of relapse after radiotherapy (41,42). Recent theoretical studies show that boosting or dose painting by numbers based on hypoxia imaging is feasible and that an increased radiation dose to the radio-resistant/hypoxic areas may result in an increased local control (43-45).

MRI

MRI provides high-resolution anatomical information with excellent soft-tissue contrast. Its use for delineation of the tumour and lymph nodes has been investigated. A major issue is obviously the movement of tumours that may cause significant artefacts. To deal with motion, two particular acquisition sequences have been useful: fast low-angle shot (FLASH) and true fast imaging with steady-state precession (TrueFISP) (46,47). Both techniques showed regular and synchronous diaphragm and chest-wall motion of diagnostic quality. Dynamic MRI can be used to define an Internal Target Volume (ITV) as it allows imaging of the entire lung volume over the breathing cycle. However, dynamic MRI scans of the lung are still prone to artefacts, which affect registration accuracy.

To the best of our knowledge, there have been no contouring studies comparing MRI to CT or FDG-PET-CT in lung cancer, neither have there been validation studies with pathology. Nevertheless, to differentiate benign from malignant nodules, Diffusion Weighted MRI (DW-MRI) may have similar accuracy as FDG-PET scans (48).

Dynamic contrast-enhanced CT (DCE-CT)

DCE-CT (or perfusion CT) imaging is a relatively new method for tumour characterization. It offers a fast way to assess functional parameters in lung cancer patients. To date DCE-CT is still a

research tool, but initial results are showing promising results for the future. DCE-CT scans give information on the blood flow (BF), blood volume (BV) and permeability of the vessels (49-52). Whereas in the literature some DCE-CT studies were hampered by the limited field-of-view (e.g., 3-5 cm) of the scanner in the cranial-caudal direction, the technical infrastructure nowadays has the ability to capture DCE-CT scans of large volumes up to 12 cm. The reproducibility of the extracted parameters of the DCE-CT scan is also within an acceptable range (49,50,53) and allows larger patient studies to look at prognostic factors for treatment outcome. These parameters are related to accessibility for chemotherapy or anti-angiogenesis drugs (54) and shown to be different between treatment responders and non-responders (53). In some series, DCE-CT extracted values correlated with prognosis and with the histological subtype of NSCLC (55). DCE-CT values give other information than FDG uptake and therefore may be complementary to characterise tumours. The clinical and prognostic implications are not yet fully understood and the number of patients who have been studied with DCE-CT is still low. Thus further clinical studies are need to assess the value of DCE-CT for the future individualized treatment and prognosis. In a recent study by Mandeville *et al.* DCE-CT parameters were evaluated in relation to markers of hypoxia (56). It was shown that BV and BF was inversely correlated to immuno-histochemical markers for hypoxia. Recently it has been shown by Lee *at al.* that reproducibility is high in DCE-CT (57). If DCE-CT is used to measure enhancement curves over time Hwang et al. could show that enhancement patterns correspond to tumor staging (58). Interestingly, looking into other body regions DCE-CT parameters might be able to predict survival, as, e.g., was shown by Koh *et al.* in patients with colorectal cancer (59). Spira *et al.* evaluated DCE-CT parameters in correlated these to histopathological findings, showing good correlation especially for microvascular density (MVD) (60). Fraioli *et al.* could demonstrate the correlation between altered perfusion parameters after treatment–indicating treatment response (61).

Dual energy CT (DECT)

Newest CT scanner technology is capable of applying two different kV setting simultaneously or rapidly after each other. The two different resulting scans can be used for tissue characterization and iodine mapping. Some studies tried to use iodine mapping for lung tumour characterization, showing initially promising results (62-64). Initial differentiation between benign and malignant pulmonary nodules seems possible, but the number of studied patients is still too low and the real clinical problem of small pulmonary nodules <8 mm currently cannot be solved sufficiently (65-67).

Imaging modalities for normal tissue characterization

Radiotherapy is always pushing the optimization of maximum tumour control with an accepted (low) level of side-effects. Radiation induced lung toxicity (RILT) is one of the major dose limiting factor in escalating the dose to lung tumours; Therefor assessment of the lung function could potentially play an important role in the design of the treatment plan. Various imaging techniques can be utilized to quantify the lung function also on a local scale, besides the general pulmonary lung function tests that only give a global assessment of the lung function.

SPECT/CT

The use of SPECT/CT for quantification of perfusion and ventilation defects in the lung is a frequently used modality for assessing lung function using imaging although the spatial resolution of the SPECT scan is limited. Radiotherapy has been shown to cause lung perfusion alterations in NSCLC patients with perfusion (68-70). Knowledge about the regional sensitivity and functioning of the lung may also guide the treatment plan design to avoid highly functioning regions inside the lung (71-74). However the hypothesis of reduced lung toxicity still has to be validated in clinical trials.

CT

CT density changes have been described after radiotherapy and show remarkable variability between patients (75,76). In depth analysis of CT characteristics of the lungs may lead to the definition of risk groups for radiation-induced lung damage.

PET/CT

The uptake of FDG in the lungs probably reflects the inflammatory status. It was found that a high FDG uptake in the lungs before radiotherapy is an independent risk factor to develop subsequent radiation pneumonitis (77). FDG-avid areas in the lungs were at the highest susceptibility for pneumonitis. Further studies are needed to elaborate on these findings before this can be used to change radiation dose distributions in the

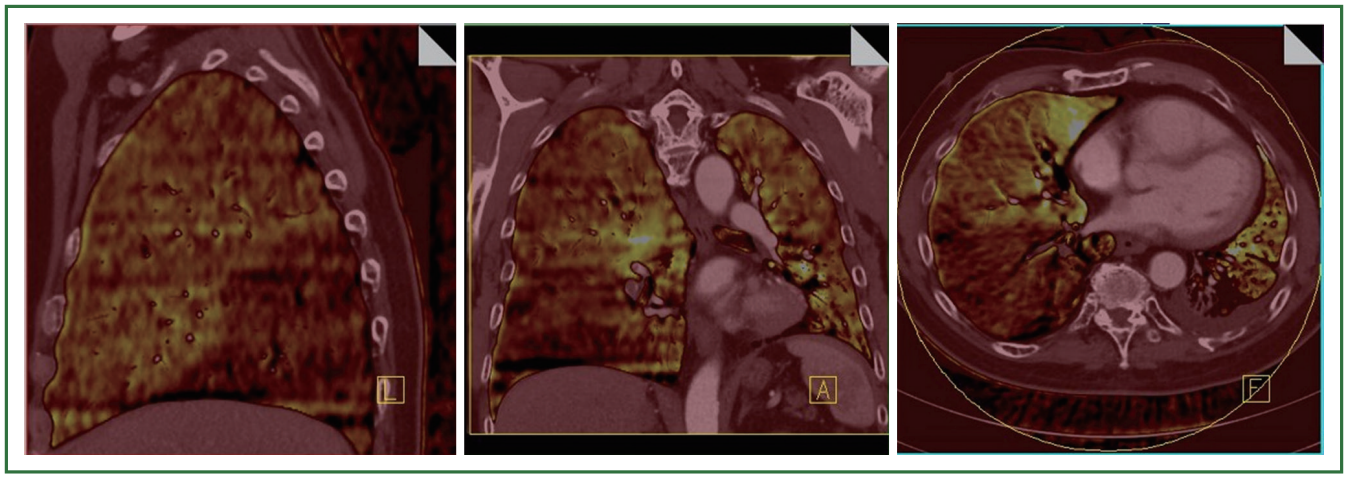

Figure 2. An example of a patient with emboli in the segmental arteries causing a large perfusion defect of the right lower lobe.

lungs on the basis of FDG uptake patterns.

MRI

MRI scans using inert hyperpolarised helium-3 gas that is inhaled by the patient show ventilated areas in the lungs (78). Non-ventilated regions do not show an MRI signal. In theoretical studies, the incorporation of this information decreased the V20 of the lungs significantly (78). However, this strategy was never investigated in prospective trials and thus remains investigational.

DECT

DECT for visualizing lung perfusion is often used in the context of the detection of pulmonary embolism (PE) (79-83). An iodine contrast material (CM) is administered and using 2 energy settings of the CT scanner (usually 80/140 kV) it is possible to visualize the distribution of iodine in the lungs. CT is the method of choice to rule out acute PE, nicely showing the emboli up to the sub-segmental level. With the use of DECT it has become possible not only to show the embolus, but also to show corresponding perfusion defects. This is of clinical importance, as was shown in earlier studies—single sub-segmental emboli (not causing significant perfusion defects) can be left untreated (84). Based on the assumption that radiation therapy of the lung may also alter CM perfusion in the lung, this technique offers potential for further assessment of patients treated for lung cancer with radiotherapy. Figure 2 shows an example of a PE in the right lower lobe causing a large perfusion defect.

While DECT is primarily used for iodine perfusion maps of the lung, Xenon ventilation consequently adds the missing part of ventilation maps for the patients. In the last years some study groups could show that the use of Xenon ventilation is feasible and safe and could also show that ventilation maps may add additional value in different pathologies such as asthma, in intensive care patients or even in children (85-93).

Treatment individualization using imaging

The next major step forward that is currently tested in clinical trials is the dose-painting hypothesis (94,95). The rationale for this is the heterogeneous nature of tumours. Differences in biological characteristics throughout tumours make them respond non-uniformly to treatment (96). Hence treatment resistant parts of the tumours are with the current homogeneous irradiation treatment techniques not optimally treated. Individualizing the treatment by using imaging information to guide or define the actual dose-response relationship is the next phase of treatment individualization (97). A currently on-going multi-centric trial in advanced NSCLC is testing the hypothesis whether a uniform dose or a boost dose to the high metabolic active volumes gives rise to better local control rates (98).

Another way of using imaging information to individualize treatment is in the context of response assessment. Using repeated imaging during treatment may provide predictive information to treatment success. Hypoxic (e.g., HX4, FAZA, FMISO), metabolic (e.g., FDG) or proliferation [e.g., FLT, (99)] PET tracers allow early in the course of treatment already an assessment of treatment (100). MRI scans can be used to evaluate changes in tumours during radiotherapy as well (101). DW-MRI derived ADC (apparent diffusion coefficient) values changes correlate well with survival. However, ADC and FDG

changes also correlate significantly. It remains unclear what the clinical value is of these predictive parameters.

With the current fractionated radiotherapy schedules in lung cancer of 4-6 weeks, there is still room for adaptation of the treatment. As previously stated, these adaptations of the treatment plan can be based either on reducing side-effects or increasing the chance of local tumour control.

Conclusions

Imaging is an integral part of target volume delineation used in current clinical practice. Tumour characterization is the next step that needs to be exploited. To fully optimize the therapeutic ratio also normal tissue toxicity is of importance. Assessment of imaging features to characterize tissue functioning should be explored as well in the context of individualized treatment optimization.

Acknowledgements

One of the authors (W.v.E.) would like to acknowledge funding (KWF MAC 2011-4970) from the Dutch Cancer Society.
Disclosure: The authors declare no conflict of interest.

References

1. Simard EP, Ward EM, Siegel R, et al. Cancers with increasing incidence trends in the United States: 1999 through 2008. CA Cancer J Clin 2012. [Epub ahead of print].
2. She J, Yang P, Hong Q, et al. Lung cancer in China: challenges and interventions. Chest 2013;143:1117-26.
3. Lagerwaard FJ, Haasbeek CJ, Smit EF, et al. Outcomes of risk-adapted fractionated stereotactic radiotherapy for stage I non-small-cell lung cancer. Int J Radiat Oncol Biol Phys 2008;70:685-92.
4. De Ruysscher D, Belderbos J, Reymen B, et al. State of the art radiation therapy for lung cancer 2012: a glimpse of the future. Clin Lung Cancer 2013;14:89-95.
5. De Ruysscher D, Wanders R, van Baardwijk A, et al. Radical treatment of non-small-cell lung cancer patients with synchronous oligometastases: long-term results of a prospective phase II trial (Nct01282450). J Thorac Oncol 2012;7:1547-55.
6. Nestle U, Kremp S, Grosu AL. Practical integration of [18F]-FDG-PET and PET-CT in the planning of radiotherapy for non-small cell lung cancer (NSCLC): the technical basis, ICRU-target volumes, problems, perspectives. Radiother Oncol 2006;81:209-25.
7. van Der Wel A, Nijsten S, Hochstenbag M, et al. Increased therapeutic ratio by 18FDG-PET CT planning in patients with clinical CT stage N2-N3M0 non-small-cell lung cancer: a modeling study. Int J Radiat Oncol Biol Phys 2005;61:649-55.
8. De Ruysscher D, Wanders S, van Haren E, et al. Selective mediastinal node irradiation based on FDG-PET scan data in patients with non-small-cell lung cancer: a prospective clinical study. Int J Radiat Oncol Biol Phys 2005;62:988-94.
9. Belderbos JS, Heemsbergen WD, De Jaeger K, et al. Final results of a Phase I/II dose escalation trial in non-small-cell lung cancer using three-dimensional conformal radiotherapy. Int J Radiat Oncol Biol Phys 2006;66:126-34.
10. van Loon J, De Ruysscher D, Wanders R, et al. Selective nodal irradiation on basis of (18)FDG-PET scans in limited-disease small-cell lung cancer: a prospective study. Int J Radiat Oncol Biol Phys 2010;77:329-36.
11. Steenbakkers RJ, Duppen JC, Fitton I, et al. Observer variation in target volume delineation of lung cancer related to radiation oncologist-computer interaction: a 'Big Brother' evaluation. Radiother Oncol 2005;77:182-90.
12. Caldwell CB, Mah K, Ung YC, et al. Observer variation in contouring gross tumor volume in patients with poorly defined non-small-cell lung tumors on CT: the impact of 18FDG-hybrid PET fusion. Int J Radiat Oncol Biol Phys 2001;51:923-31.
13. Werner-Wasik M, Nelson AD, Choi W, et al. What is the best way to contour lung tumors on PET scans? Multiobserver validation of a gradient-based method using a NSCLC digital PET phantom. Int J Radiat Oncol Biol Phys 2012;82:1164-71.
14. Thorwarth D, Beyer T, Boellaard R, et al. Integration of FDG-PET/CT into external beam radiation therapy planning: technical aspects and recommendations on methodological approaches. Nuklearmedizin 2012;51:140-53.
15. Nehmeh SA, Erdi YE, Ling CC, et al. Effect of respiratory gating on quantifying PET images of lung cancer. J Nucl Med 2002;43:876-81.
16. Aristophanous M, Berbeco RI, Killoran JH, et al. Clinical utility of 4D FDG-PET/CT scans in radiation treatment planning. Int J Radiat Oncol Biol Phys 2012;82:e99-105.
17. García Vicente AM, Soriano Castrejon AM, Talavera Rubio MP, et al. (18)F-FDG PET-CT respiratory gating in characterization of pulmonary lesions: approximation towards clinical indications. Ann Nucl Med 2010;24:207-14.
18. Dawood M, Buther F, Lang N, et al. Respiratory gating in positron emission tomography: a quantitative comparison of different gating schemes. Med Phys 2007;34:3067-76.
19. Liu C, Alessio A, Pierce L, et al. Quiescent period respiratory gating for PET/CT. Med Phys 2010;37:5037-43.
20. van Elmpt W, Hamill J, Jones J, et al. Optimal gating compared to 3D and 4D PET reconstruction for characterization of lung tumours. Eur J Nucl Med Mol Imaging 2011;38:843-55.
21. Dawood M, Lang N, Jiang X, et al. Lung motion correction on respiratory gated 3-D PET/CT images. IEEE Trans Med Imaging 2006;25:476-85.
22. van Baardwijk A, Bosmans G, Boersma L, et al. PET-CT-based auto-contouring in non-small-cell lung cancer correlates with pathology and

reduces interobserver variability in the delineation of the primary tumor and involved nodal volumes. Int J Radiat Oncol Biol Phys 2007;68:771-8.
23. Bayne M, Hicks RJ, Everitt S, et al. Reproducibility of "intelligent" contouring of gross tumor volume in non-small-cell lung cancer on PET/CT images using a standardized visual method. Int J Radiat Oncol Biol Phys 2010;77:1151-7.
24. van Loon J, Siedschlag C, Stroom J, et al. Microscopic disease extension in three dimensions for non-small-cell lung cancer: development of a prediction model using pathology-validated positron emission tomography and computed tomography features. Int J Radiat Oncol Biol Phys 2012;82:448-56.
25. Schaefer A, Kim YJ, Kremp S, et al. PET-based delineation of tumour volumes in lung cancer: comparison with pathological findings. Eur J Nucl Med Mol Imaging 2013;40:1233-44.
26. Cheebsumon P, Boellaard R, de Ruysscher D, et al. Assessment of tumour size in PET/CT lung cancer studies: PET- and CT-based methods compared to pathology. EJNMMI Res 2012;2:56.
27. Hatt M, Cheze-le Rest C, van Baardwijk A, et al. Impact of tumor size and tracer uptake heterogeneity in (18)F-FDG PET and CT non-small cell lung cancer tumor delineation. J Nucl Med 2011;52:1690-7.
28. Stroom J, Blaauwgeers H, van Baardwijk A, et al. Feasibility of pathology-correlated lung imaging for accurate target definition of lung tumors. Int J Radiat Oncol Biol Phys 2007;69:267-75.
29. Zaidi H, El Naqa I. PET-guided delineation of radiation therapy treatment volumes: a survey of image segmentation techniques. Eur J Nucl Med Mol Imaging 2010;37:2165-87.
30. Lee JA. Segmentation of positron emission tomography images: some recommendations for target delineation in radiation oncology. Radiother Oncol 2010;96:302-7.
31. Wouters BG, van den Beucken T, Magagnin MG, et al. Targeting hypoxia tolerance in cancer. Drug Resist Updat 2004;7:25-40.
32. Bollineni VR, Wiegman EM, Pruim J, et al. Hypoxia imaging using Positron Emission Tomography in non-small cell lung cancer: implications for radiotherapy. Cancer Treat Rev 2012;38:1027-32.
33. Mees G, Dierckx R, Vangestel C, et al. Molecular imaging of hypoxia with radiolabelled agents. Eur J Nucl Med Mol Imaging 2009;36:1674-86.
34. Thorwarth D, Eschmann SM, Scheiderbauer J, et al. Kinetic analysis of dynamic 18F-fluoromisonidazole PET correlates with radiation treatment outcome in head-and-neck cancer. BMC Cancer 2005;5:152.
35. Cherk MH, Foo SS, Poon AM, et al. Lack of correlation of hypoxic cell fraction and angiogenesis with glucose metabolic rate in non-small cell lung cancer assessed by 18F-Fluoromisonidazole and 18F-FDG PET. J Nucl Med 2006;47:1921-6.
36. Bollineni VR, Kerner GS, Pruim J, et al. PET imaging of tumor hypoxia using 18F-Fluoroazomycin arabinoside in stage III-IV non-small cell lung cancer patients. J Nucl Med 2013;54:1175-80.
37. Li L, Hu M, Zhu H, et al. Comparison of 18F-Fluoroerythronitroimidazole and 18F-fluorodeoxyglucose positron emission tomography and prognostic value in locally advanced non-small-cell lung cancer. Clin Lung Cancer 2010;11:335-40.
38. Gagel B, Reinartz P, Demirel C, et al. [18F] fluoromisonidazole and [18F] fluorodeoxyglucose positron emission tomography in response evaluation after chemo-/radiotherapy of non-small-cell lung cancer: a feasibility study. BMC Cancer 2006;6:51.
39. Postema EJ, McEwan AJ, Riauka TA, et al. Initial results of hypoxia imaging using 1-alpha-D: -(5-deoxy-5-[18F]-fluoroarabinofuranosyl)-2-nitroimidazole (18F-FAZA). Eur J Nucl Med Mol Imaging 2009;36:1565-73.
40. Koh WJ, Bergman KS, Rasey JS, et al. Evaluation of oxygenation status during fractionated radiotherapy in human nonsmall cell lung cancers using [F-18]fluoromisonidazole positron emission tomography. Int J Radiat Oncol Biol Phys 1995;33:391-8.
41. Eschmann SM, Paulsen F, Reimold M, et al. Prognostic impact of hypoxia imaging with 18F-misonidazole PET in non-small cell lung cancer and head and neck cancer before radiotherapy. J Nucl Med 2005;46:253-60.
42. Dehdashti F, Mintun MA, Lewis JS, et al. In vivo assessment of tumor hypoxia in lung cancer with 60Cu-ATSM. Eur J Nucl Med Mol Imaging 2003;30:844-50.
43. Thorwarth D, Eschmann SM, Paulsen F, et al. Hypoxia dose painting by numbers: a planning study. International journal of radiation oncology, biology, physics 2007;68:291-300.
44. Hendrickson K, Phillips M, Smith W, et al. Hypoxia imaging with [F-18] FMISO-PET in head and neck cancer: potential for guiding intensity modulated radiation therapy in overcoming hypoxia-induced treatment resistance. Radiother Oncol 2011;101:369-75.
45. Thorwarth D, Alber M. Implementation of hypoxia imaging into treatment planning and delivery. Radiother Oncol 2010;97:172-5.
46. Plathow C, Klopp M, Fink C, et al. Quantitative analysis of lung and tumour mobility: comparison of two time-resolved MRI sequences. Br J Radiol 2005;78:836-40.
47. Blackall JM, Ahmad S, Miquel ME, et al. MRI-based measurements of respiratory motion variability and assessment of imaging strategies for radiotherapy planning. Phys Med Biol 2006;51:4147-69.
48. Mori T, Nomori H, Ikeda K, et al. Diffusion-weighted magnetic resonance imaging for diagnosing malignant pulmonary nodules/masses: comparison with positron emission tomography. J Thorac Oncol 2008;3:358-64.
49. Ng QS, Goh V, Fichte H, et al. Lung cancer perfusion at multi-detector row CT: reproducibility of whole tumor quantitative measurements. Radiology 2006;239:547-53.
50. Ng QS, Goh V, Milner J, et al. Acute tumor vascular effects following fractionated radiotherapy in human lung cancer: in vivo whole tumor assessment using volumetric perfusion computed tomography. Int J Radiat Oncol Biol Phys 2007;67:417-24.
51. Miles KA, Griffiths MR. Perfusion CT: a worthwhile enhancement? Br J Radiol 2003;76:220-31.
52. Miles KA, Griffiths MR, Fuentes MA. Standardized perfusion value: universal CT contrast enhancement scale that correlates with FDG PET in

lung nodules. Radiology 2001;220:548-53.

53. Wang J, Wu N, Cham MD, et al. Tumor response in patients with advanced non-small cell lung cancer: perfusion CT evaluation of chemotherapy and radiation therapy. AJR Am J Roentgenol 2009;193:1090-6.
54. Lazanyi KS, Abramyuk A, Wolf G, et al. Usefulness of dynamic contrast enhanced computed tomography in patients with non-small-cell lung cancer scheduled for radiation therapy. Lung Cancer 2010;70:280-5.
55. Shastry M, Miles KA, Win T, et al. Integrated 18F-fluorodeoxyglucose-positron emission tomography/dynamic contrast-enhanced computed tomography to phenotype non-small cell lung carcinoma. Mol Imaging 2012;11:353-60.
56. Mandeville HC, Ng QS, Daley FM, et al. Operable non-small cell lung cancer: correlation of volumetric helical dynamic contrast-enhanced CT parameters with immunohistochemical markers of tumor hypoxia. Radiology 2012;264:581-9.
57. Lee SM, Lee HJ, Kim JI, et al. Adaptive 4D volume perfusion CT of lung cancer: effects of computerized motion correction and the range of volume coverage on measurement reproducibility. AJR Am J Roentgenol 2013;200:W603-9.
58. Hwang SH, Yoo MR, Park CH, et al. Dynamic contrast-enhanced CT to assess metabolic response in patients with advanced non-small cell lung cancer and stable disease after chemotherapy or chemoradiotherapy. Eur Radiol 2013;23:1573-81.
59. Koh TS, Ng QS, Thng CH, et al. Primary colorectal cancer: use of kinetic modeling of dynamic contrast-enhanced CT data to predict clinical outcome. Radiology 2013;267:145-54.
60. Spira D, Neumeister H, Spira SM, et al. Assessment of tumor vascularity in lung cancer using volume perfusion CT (VPCT) with histopathologic comparison: a further step toward an individualized tumor characterization. J Comput Assist Tomogr 2013;37:15-21.
61. Fraioli F, Anzidei M, Zaccagna F, et al. Whole-tumor perfusion CT in patients with advanced lung adenocarcinoma treated with conventional and antiangiogenetic chemotherapy: initial experience. Radiology 2011;259:574-82.
62. Schmid-Bindert G, Henzler T, Chu TQ, et al. Functional imaging of lung cancer using dual energy CT: how does iodine related attenuation correlate with standardized uptake value of 18FDG-PET-CT? Eur Radiol 2012;22:93-103.
63. Kim YN, Lee HY, Lee KS, et al. Dual-energy CT in patients treated with anti-angiogenic agents for non-small cell lung cancer: new method of monitoring tumor response? Korean J Radiol 2012;13:702-10.
64. Zhang LJ, Yang GF, Wu SY, et al. Dual-energy CT imaging of thoracic malignancies. Cancer Imaging 2013;13:81-91.
65. Chae EJ, Song JW, Krauss B, et al. Dual-energy computed tomography characterization of solitary pulmonary nodules. J Thorac Imaging 2010;25:301-10.
66. Goodsitt MM, Chan HP, Way TW, et al. Quantitative CT of lung nodules: dependence of calibration on patient body size, anatomic region, and calibration nodule size for single- and dual-energy techniques. Med Phys 2009;36:3107-21.
67. Chae EJ, Song JW, Seo JB, et al. Clinical utility of dual-energy CT in the evaluation of solitary pulmonary nodules: initial experience. Radiology 2008;249:671-81.
68. Scheenstra AE, Rossi MM, Belderbos JS, et al. Local dose-effect relations for lung perfusion post stereotactic body radiotherapy. Radiother Oncol 2013;107:398-402.
69. De Jaeger K, Seppenwoolde Y, Boersma LJ, et al. Pulmonary function following high-dose radiotherapy of non-small-cell lung cancer. Int J Radiat Oncol Biol Phys 2003;55:1331-40.
70. Zhang J, Ma J, Zhou S, et al. Radiation-induced reductions in regional lung perfusion: 0.1-12 year data from a prospective clinical study. Int J Radiat Oncol Biol Phys 2010;76:425-32.
71. St-Hilaire J, Lavoie C, Dagnault A, et al. Functional avoidance of lung in plan optimization with an aperture-based inverse planning system. Radiother Oncol 2011;100:390-5.
72. Munawar I, Yaremko BP, Craig J, et al. Intensity modulated radiotherapy of non-small-cell lung cancer incorporating SPECT ventilation imaging. Med Phys 2010;37:1863-72.
73. McGuire SM, Marks LB, Yin FF, et al. A methodology for selecting the beam arrangement to reduce the intensity-modulated radiation therapy (IMRT) dose to the SPECT-defined functioning lung. Phys Med Biol 2010;55:403-16.
74. Lavrenkov K, Singh S, Christian JA, et al. Effective avoidance of a functional spect-perfused lung using intensity modulated radiotherapy (IMRT) for non-small cell lung cancer (NSCLC): an update of a planning study. Radiother Oncol 2009;91:349-52.
75. De Ruysscher D, Sharifi H, Defraene G, et al. Quantification of radiation-induced lung damage with CT scans: the possible benefit for radiogenomics. Acta Oncol 2013;52:1405-10.
76. Ghobadi G, Hogeweg LE, Faber H, et al. Quantifying local radiation-induced lung damage from computed tomography. Int J Radiat Oncol Biol Phys 2010;76:548-56.
77. Petit SF, van Elmpt WJ, Oberije CJ, et al. [18F]fluorodeoxyglucose uptake patterns in lung before radiotherapy identify areas more susceptible to radiation-induced lung toxicity in non-small-cell lung cancer patients. Int J Radiat Oncol Biol Phys 2011;81:698-705.
78. Ireland RH, Bragg CM, McJury M, et al. Feasibility of image registration and intensity-modulated radiotherapy planning with hyperpolarized helium-3 magnetic resonance imaging for non-small-cell lung cancer. Int J Radiat Oncol Biol Phys 2007;68:273-81.
79. Zhang LJ, Zhou CS, Schoepf UJ, et al. Dual-energy CT lung ventilation/perfusion imaging for diagnosing pulmonary embolism. Eur Radiol 2013;23:2666-75.
80. Tang CX, Zhang LJ, Han ZH, et al. Dual-energy CT based vascular iodine analysis improves sensitivity for peripheral pulmonary artery thrombus detection: An experimental study in canines. Eur J Radiol 2013;82:2270-8.

81. Hansmann J, Fink C, Jost G, et al. Impact of iodine delivery rate with varying flow rates on image quality in dual-energy CT of patients with suspected pulmonary embolism. Acad Radiol 2013;20:962-71.
82. Nagayama H, Sueyoshi E, Hayashida T, et al. Quantification of lung perfusion blood volume (lung PBV) by dual-energy CT in pulmonary embolism before and after treatment: preliminary results. Clin Imaging 2013;37:493-7.
83. Yuan R, Shuman WP, Earls JP, et al. Reduced iodine load at CT pulmonary angiography with dual-energy monochromatic imaging: comparison with standard CT pulmonary angiography--a prospective randomized trial. Radiology 2012;262:290-7.
84. Apfaltrer P, Bachmann V, Meyer M, et al. Prognostic value of perfusion defect volume at dual energy CTA in patients with pulmonary embolism: correlation with CTA obstruction scores, CT parameters of right ventricular dysfunction and adverse clinical outcome. Eur J Radiol 2012;81:3592-7.
85. Kim WW, Lee CH, Goo JM, et al. Xenon-enhanced dual-energy CT of patients with asthma: dynamic ventilation changes after methacholine and salbutamol inhalation. AJR Am J Roentgenol 2012;199:975-81.
86. Honda N, Osada H, Watanabe W, et al. Imaging of ventilation with dual-energy CT during breath hold after single vital-capacity inspiration of stable xenon. Radiology 2012;262:262-8.
87. Hoegl S, Meinel FG, Thieme SF, et al. Worsening respiratory function in mechanically ventilated intensive care patients: feasibility and value of xenon-enhanced dual energy CT. Eur J Radiol 2013;82:557-62.
88. Yanagita H, Honda N, Nakayama M, et al. Prediction of postoperative pulmonary function: preliminary comparison of single-breath dual-energy xenon CT with three conventional methods. Jpn J Radiol 2013;31:377-85.
89. Goo HW, Yu J. Redistributed regional ventilation after the administration of a bronchodilator demonstrated on xenon-inhaled dual-energy CT in a patient with asthma. Korean J Radiol 2011;12:386-9.
90. Goo HW, Yang DH, Hong SJ, et al. Xenon ventilation CT using dual-source and dual-energy technique in children with bronchiolitis obliterans: correlation of xenon and CT density values with pulmonary function test results. Pediatr Radiol 2010;40:1490-7.
91. Chae EJ, Seo JB, Lee J, et al. Xenon ventilation imaging using dual-energy computed tomography in asthmatics: initial experience. Invest Radiol 2010;45:354-61.
92. Chae EJ, Seo JB, Goo HW, et al. Xenon ventilation CT with a dual-energy technique of dual-source CT: initial experience. Radiology 2008;248:615-24.
93. Goo HW, Chae EJ, Seo JB, et al. Xenon ventilation CT using a dual-source dual-energy technique: dynamic ventilation abnormality in a child with bronchial atresia. Pediatr Radiol 2008;38:1113-6.
94. Bentzen SM. Theragnostic imaging for radiation oncology: dose-painting by numbers. Lancet Oncol 2005;6:112-7.
95. Ling CC, Humm J, Larson S, et al. Towards multidimensional radiotherapy (MD-CRT): biological imaging and biological conformality. Int J Radiat Oncol Biol Phys 2000;47:551-60.
96. Lambin P, van Stiphout RG, Starmans MH, et al. Predicting outcomes in radiation oncology--multifactorial decision support systems. Nat Rev Clin Oncol 2013;10:27-40.
97. Lambin P, Petit SF, Aerts HJ, et al. The ESTRO Breur Lecture 2009. From population to voxel-based radiotherapy: exploiting intra-tumour and intra-organ heterogeneity for advanced treatment of non-small cell lung cancer. Radiother Oncol 2010;96:145-52.
98. van Elmpt W, De Ruysscher D, van der Salm A, et al. The PET-boost randomised phase II dose-escalation trial in non-small cell lung cancer. Radiother Oncol 2012;104:67-71.
99. Everitt S, Hicks RJ, Ball D, et al. Imaging cellular proliferation during chemo-radiotherapy: a pilot study of serial 18F-FLT positron emission tomography/computed tomography imaging for non-small-cell lung cancer. Int J Radiat Oncol Biol Phys 2009;75:1098-104.
100. van Elmpt W, Ollers M, Dingemans AM, et al. Response assessment using 18F-FDG PET early in the course of radiotherapy correlates with survival in advanced-stage non-small cell lung cancer. J Nucl Med 2012;53:1514-20.
101. Tsuchida T, Morikawa M, Demura Y, et al. Imaging the early response to chemotherapy in advanced lung cancer with diffusion-weighted magnetic resonance imaging compared to fluorine-18 fluorodeoxyglucose positron emission tomography and computed tomography. J Magn Reson Imaging 2013;38:80-8.

Cite this article as: van Elmpt W, Zegers CM, Das M, De Ruysscher D. Imaging techniques for tumour delineation and heterogeneity quantification of lung cancer: overview of current possibilities. J Thorac Dis 2014;6(4):319-327. doi: 10.3978/j.issn.2072-1439.2013.08.62